Journal of Solid Mechanics Vol. 13, No. 4 (2021) pp. 399-412
DOI: 10.22034/jsm.2020.1900703.1594

Buckling and Free Vibrations of a Magneto-Electro-Elastic Sandwich Panel with Flexible Core

H. Talebi Amanieh, S.A. Seyed Roknizadeh *, A. Reza

Department of Mechanical Engineering, Ahvaz Branch, Islamic Azad University, Ahvaz, Iran

Received 8 July 2021; accepted 13 September 2021

ABSTRACT

This paper presents the buckling and out-of-plane free vibration response of a sandwich panel with flexible core for the different boundary condition. In the desired configuration of the sandwich panel, the top and bottom plates are made of magneto-electro-elastic (MEE) plates. Moreover, the in-plane electric and magnetic potential fields are neglected for the derivation of the required relations. The sandwich structure is subjected to axial force in both longitudinal and transverse directions; in addition, and the top and bottom plates are exposed to electric and magnetic fields. The governing equations of motion for MEE sandwich panel with a flexible core are derived based on the first-order shear deformation theory by neglecting the displacement of the mid-plate and using the Hamilton's principle. Furthermore, the derived partial differential equations (PDEs) are solved. According to the obtained numerical results, the core thickness, variation of electric field, variation of magnetic field and plate length are introduced as the most influential parameters on the free vibration response of the panel as well as the critical force of buckling. As one of the results, the electric potential is inversely related to the natural frequency and buckling load, so that with increasing the electric potential, the natural frequency and critical load of the structure is also increased. Moreover, the magnetic potential is directly related to the natural frequency and buckling load of the system, and increasing trends of natural frequency and critical load are observed by increasing the magnetic potential.

© 2021 IAU, Arak Branch.All rights reserved.

Keywords : Buckling; Out-of-plane free vibrations; Sandwich panel; Magneto-electro-elastic plate; Flexible core.

1 INTRODUCTION

NOWADAYS, regarding the advances in various sciences and industries, the need for light, durable and intelligent structures is of great significance. Regarding the light weight and high flexibility features of the sandwich structures with flexible cores, they have been introduced as an efficient solution for controlling and reducing the vibrations of the structure. Consequently, much attentions have been dedicated to the study of buckling and vibration of such structures. Besides the provision of high strength and low weight by MEE sandwich panels with

*Corresponding author. Tel.: +98 6133348420-4, Fax.: +98 6133329200.
E-mail address: s.roknizadeh@scu.ac.ir (S.A. Seyed Roknizadeh)

© 2021 IAU, Arak Branch. All rights reserved.

flexible cores, the ability to convert mechanical, electrical and magnetic energies into each other is considered as other advantageous feature of these structures. Sandwich panels are extensively used in various industrial, aerospace and space applications due to their high bending strength and low weight. In the mid-1960s, several investigations were conducted on such panels. In some studies [1, 2] analytical and numerical approaches for sandwich panels and numerical solutions for standard problems were presented. Rouhani and Marceller [3] studied the vibrations and buckling of a rectangular sandwich plate with a small displacement theory for different types of support conditions. The Reighley-Ritz method was utilized for solving the equations and the enhanced importance of support conditions on buckling and vibration in higher aspect ratios was declared. For better evaluation of buckling and vibrations in a sandwich panel with a flexible core, Frostig and Thompson [4, 5] presented two comprehensive models for modeling a flexible core. In the prior model, normal shear stress was used in the core; while in the latter model, the core displacements were assumed in the polynomial form. A good agreement with the first and higher-order deformation theories was achieved by the presented models. The use of Galerkin method and higher-order deformation theories for studying the vibrations of a sandwich plate with a flexible core was presented by Schwartz Giuli et al. [6, 7]. In their approach, the core was modeled with polynomial functions, known as Frostig model. Generally, two types of core modeling have been performed; non-contact assumption with the surface and consideration of contact with the surface. Comparing the results of these modeling, the main role of the contact conditions in natural frequency and mode shape was deduced. In another study by Frostig and Thompson [8, 9], the vibrations of a sandwich panel with a flexible core and temperature-dependent properties were analyzed. In this study, the governing equations of motion were extracted based on the higher-order shear deformation theory and Hamilton's principle. Moreover, two types of temperature distribution were considered in the core; uniform temperature variation along the core thickness and a linear temperature variation along the thickness. Their results declared the reduced frequency as a result of increasing temperature or temperature gradient. Arajo et al. [10] modeled the vibrations of a sandwich panel consisting of two layers of composite, flexible core and two layers of piezoelectric plate as sensors and actuators by the finite element method. They demonstrated the impact of the flexible core on control feedback and the importance of core modeling in the active control of the structure. The dynamic response of composite sandwich panels on the elastic foundation subjected to the impact loading was assessed by Malekzadeh Fard et al.[11].The first-order shear deformation theory was implemented for the derivation of relations for faces; in addition, the core was modeled through Frostig theory. Moreover, the effects of elastic foundation on the vibrations of sandwich panels as well as effect of impact loading at the center of the plate were investigated. In another article Malekzadeh Fard and Malek-Mohammadi [12] investigated free vibrations and buckling of the sandwich panels with composite skin layers and flexible core using Frostig's first theory for modeling core. The main advantage of this theory is its simplicity and less number of equations than the second method of Frostig's high-order theory. Daikh et al. [13]studied the vibrations of a nanoscale sandwich panels with a functionally graded core in a thermal environment. Relationships were extracted on the basis of Eringen's nonlocal theory and the higher-order shear deformation theory, and the solutions of the governing equations were determined using the Navier's approach. The results show the effect of temperature, power index and nano parameters on the dimensionless natural frequency of the sandwich panel. For achieving better consistency with the experimental results, Jam et al. [14]considered the in-plane stresses of the core in analyzing the vibrations of a sandwich panel with a flexible core. Furthermore, Mohammadi Mehr and Mostafavifar [15] studied the vibrations of a sandwich panel with a flexible core, top and bottom layers of functionally graded nanocarbon under longitudinal magnetic field. A comprehensive review on the vibrations and buckling of sandwich panels was surveyed by Kumar and Serinoasa[16]. They declared the insufficient study on the field of sandwich panels with functionally graded and smart faces. Several investigations have been performed concerning the vibrations of MEE plates. Among these investigations, it can be mentioned to the work of Pan and Hiliger [17], in which the linear vibrations of multilayer rectangular MEE plate with simply supported boundary conditions were investigated. The governing equations were derived through the thin plate theory (classical plate theory), and the natural frequencies and mode shapes were calculated using the propagator matrix method. Buchanan [18] examined and compared the free vibrations of a multilayer plate with a multi-phase MEE plate. The frequency responses were presented by obtaining the shape functions using the Galerkin method through the application of finite element method and considering the 3-node elements. Chen et al. [19] examined the free vibrations of the non-homogeneous transversely isotropic MEE plate with a simply supported edges. They extracted three-dimensional (3-D) equilibrium equations of the plate and solved the problem numerically. Ramirez et al. [20] examined the response to 2-D free vibration of MEE multilayer plates. The intended model was independent of boundary conditions and the approximate solution of the problem was achieved by combining the discrete layer approach and Ritz method. The exact vibrations solution of a transversely isotropic thin rectangular MEE plate was presented by Liu and Chang [21] for the first time. In this paper, free vibrations of two-layered BaTiO3-CoFe2O4 composite material was obtained and the effect of different

© 2021 IAU, Arak Branch

volume fraction on natural frequency was investigated. Davi and Millazzo [22]surveyed the free vibrations of the MEE structure by the mesh less method. Milazzo and Orlando [23]examined the exact solution of free vibrations in a multi-layered MEE plate with the third-order shear deformation theory (Reddy'**s** theory). Chang [24, 25] solved the random vibrations and natural frequencies of a MEE rectangular plate in collision with a fluid by increasing the virtual mass for different support conditions. In this study, incompressible, inviscid and non-rotating assumptions were considered for the fluid. In another study by Chen et al. [26], the 3-D free vibrations of a multi-layer MEE plate under clamped-free support conditions with an approximation method of a discrete layer approach was studied. The intelligent control of nonlinear vibrations of MEE rectangular plates was investigated by Katimani and Ray [27].In this study, the active damping analysis of the compressed layer was studied through Golla's model. Liaoling et al. [28] examined the free vibrations of nano-MEE on the basis of non-local theory. In the mentioned investigation, the classical plate theory with simply supported boundary conditions and non-local Eringen's theory were implemented. External electric potential, external magnetic potential and temperature were applied to the plate and the derived equations of motion were solved through Navier's approach. The free vibrations of MEE plate on elastic substrate was studied by Li and Zhang [29] using the first-order shear deformation theory (Mindlin's theory) and neglecting the in-plane electric and magnetic fields. In another investigation, the buckling of MEE plate on Pasternak foundation was investigated by Li [30] through the use of first-order shear deformation theory. Karimi et al [31-33] investigated the effects of surface energy layers/stress on bending/buckling and vibration analysis of METE Nano plates. The refined plate theory, surface energy, nonlocal hypotheses and the Hamilton principle were employed to derive the governing equations of motion for the double layer magneto-electro-thermo-elastic Nano plates, then the Galerkin method was employed to solve the governing equations. Effects of some parameters such as external electric/ magnetic potentials, elastic foundations, skew angle, and temperature change on surface properties were investigated. Motivation and objective of this work. Proper evaluation of MEE material's behavior as a new class of smart materials which have coupling interaction among electrical, magnetic, and mechanical fields is necessary. Actually for improving our understanding about these materials it is necessary to analyze them in different structures with more accurate assumptions. By reviewing the previous investigations, it has been found that, the out-of-plane free vibrations and buckling of the MEE sandwich panels with a flexible core based on the first-order shear deformation theory and different boundary conditions such as SSSS, CCCC and SSCC have not been studied so far.

Accordingly, in this paper, an effort is made to find what effects could have the flexible core and other influential parameters on the buckling and vibration of the MEE sandwich panels. The investigation is conducted by the neglecting of mid-plates displacements as well as electric and magnetic fields within the plate. The upper and lower plates are also subjected to electrical and magnetic fields. The governing equations of motion are extracted by considering the normal and shear stresses for the core and the implementation of Hamilton's principle. Then the derived PDEs would be solved by analytic solution method. The investigation could be appropriate for various industrial, aerospace and space applications due to their high bending strength, low weight and intelligent materials.

2 PROBLEM MODELING

A MEE sandwich panel with a length of a, width of b and thickness of h, with simply supported edges is considered as depicted in Fig. 1. The panel is consisted of three layers; the top and bottom layers made of MEE with the respective thicknesses of h_t and h_b , and the flexible core of foam with the thickness of h_c .

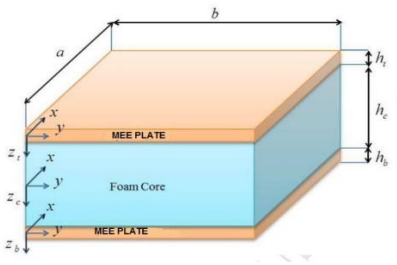

Fig.1
The MEE sandwich panel with flexible core.

According to the first-order shear deformation theory, with the neglection of mid-plates displacements of the sandwich panel, the relations for the displacement sandwich panel can be expressed as follows [29]:

© 2021 IAU, Arak Branch

$$
\begin{aligned}
&u^i(x,y,z,t) = z\,\theta_x^i(x,y,t)\\
&v^i(x,y,z,t) = z\,\theta_y^i(x,y,t)\\
&w(x,y,z,t) = w_0(x,y,t) \qquad i = b,c,t
\end{aligned} \tag{1}
$$

where, θ_x and θ_y represent the normal transverse rotations with respect to x and y axes, respectively. In addition, considering the continuity between the layers, the core rotations can be obtained as:

$$
\theta_x^c = -\frac{1}{h_c}\left(\frac{h_b}{2}\theta_x^b + \frac{h_t}{2}\theta_x^t\right) \qquad \theta_y^c = -\frac{1}{h_c}\left(\frac{h_b}{2}\theta_y^b + \frac{h_t}{2}\theta_y^t\right) \tag{2}
$$

According to the above displacement relations, the linear strains for the rectangular sandwich panel are stated as follows [29]:

$$
\begin{aligned}
&\varepsilon_x^i = u_{,x} = u^i_{0,x} + z\,\theta^i_{x,x}\\
&\varepsilon_y^i = v_{,y} = v^i_{0,y} + z\,\theta^i_{y,y}\\
&\gamma_{xz}^i = u_{,z} + w_{,x} = k\,(w_{0,x} + \theta_x^i) \qquad i = b,c,t\\
&\gamma_{yz}^i = v_{,z} + w_{,y} = k\,(w_{0,y} + \theta_y^i)\\
&\gamma_{xy}^i = u_{,y} + v_{,x} = u^i_{0,y} + v^i_{0,x} + z\,(\theta^i_{x,y} + \theta^i_{y,x})
\end{aligned} \tag{3}
$$

The structural equations functionally graded MEE plate are expressed in the following form [29]:

$$
\sigma = c\varepsilon - eE - qH \qquad D = e^T\varepsilon + \eta E + dH \qquad B = q^T\varepsilon + dE + \mu H \tag{4}
$$

where, σ and ε denote the stress and strain, D is the electric displacement, B is the magnetic flux vector, E is the electric field, H is the magnetic field vector, C is the elastic coefficient, η is the dielectric coefficient, μ is the magnetic coefficient, e is piezoelectric, q is piezomagnetic, and d is magneto-electric coefficient.

The coefficients of the structural equation are defined as follows [29]:

$$
C = \begin{bmatrix} c_{11} & c_{12} & 0 & 0 & 0\\ c_{12} & c_{22} & 0 & 0 & 0\\ 0 & 0 & c_{44} & 0 & 0\\ 0 & 0 & 0 & c_{55} & 0\\ 0 & 0 & 0 & 0 & c_{66} \end{bmatrix} \qquad e = \begin{bmatrix} 0 & 0 & e_{31}\\ 0 & 0 & e_{32}\\ 0 & e_{24} & 0\\ e_{15} & 0 & 0\\ 0 & 0 & 0 \end{bmatrix}
$$

$$
d = \begin{bmatrix} d_{11} & 0 & 0\\ 0 & d_{22} & 0\\ 0 & 0 & d_{33} \end{bmatrix} \qquad q = \begin{bmatrix} 0 & 0 & q_{31}\\ 0 & 0 & q_{32}\\ 0 & q_{24} & 0\\ q_{15} & 0 & 0\\ 0 & 0 & 0 \end{bmatrix} \tag{5}
$$

$$
\eta = \begin{bmatrix} \eta_{11} & 0 & 0\\ 0 & \eta_{22} & 0\\ 0 & 0 & \eta_{33} \end{bmatrix} \qquad \mu = \begin{bmatrix} \mu_{11} & 0 & 0\\ 0 & \mu_{22} & 0\\ 0 & 0 & \mu_{33} \end{bmatrix}
$$

The top and bottom layers of the MEE sandwich panel along z axis affected by the electric potential of ϕ_0 and the magnetic potential of ψ_0 are located between the top and bottom surfaces of each layer. The electrical and magnetic boundary conditions of the plate surface are expressed in the following form [28]:

© 2021 IAU, Arak Branch

$$\begin{aligned}&\Phi(x,y,-\frac{h_i}{2},t)=-\phi_0\ ,\ \Phi(x,y,\frac{h_i}{2},t)=\phi_0\\&\Psi(x,y,-\frac{h_i}{2},t)=-\psi_0\ ,\ \Psi(x,y,\frac{h_i}{2},t)=\psi_0\qquad i=t,b\end{aligned}\tag{6}$$

If the electric vector and the magnetic field intensity are defined as the scalar gradients of electric and magnetic potential of ϕ and ψ , respectively, the Maxwell's equations in quasi-static approximation are satisfied.

$$\begin{aligned}&E=-\nabla\phi\\&H=-\nabla\psi\end{aligned}\tag{7}$$

3 EQUATIONS OF MOTION

The governing differential equations of motion on the basis of first-order shear deformation theory for MEE sandwich plates considering normal and shear stresses for a flexible core can be obtained using the Hamilton's principle, which are defined as follows:

$$\begin{aligned}&\delta\theta_x^b: M^b_{x,x}+M^b_{xy,y}-Q_x^b+\frac{h_b}{2h_c}Q_x^c-\frac{h_b}{2h_c}M^c_{x,x}-\frac{h_b}{2h_c}M^c_{xy,y}=I_2^b\ddot{\theta}_x^b-\frac{h_b}{2h_c}I_2^c\ddot{\theta}_x^c\\&\delta\theta_y^b: M^b_{y,y}+M^b_{xy,x}-Q_y^b+\frac{h_b}{2h_c}Q_y^c-\frac{h_b}{2h_c}M^c_{y,y}-\frac{h_b}{2h_c}M^c_{xy,x}=I_2^b\ddot{\theta}_y^b-\frac{h_b}{2h_c}I_2^c\ddot{\theta}_y^c\\&\delta\theta_x^t: M^t_{x,x}+M^t_{xy,y}-Q_x^t+\frac{h_t}{2h_c}Q_x^c-\frac{h_t}{2h_c}M^c_{x,x}-\frac{h_t}{2h_c}M^c_{xy,y}=I_2^t\ddot{\theta}_x^t-\frac{h_t}{2h_c}I_2^c\ddot{\theta}_x^c\\&\delta\theta_y^t: M^t_{y,y}+M^t_{xy,x}-Q_y^t+\frac{h_t}{2h_c}Q_y^c-\frac{h_t}{2h_c}M^c_{y,y}-\frac{h_t}{2h_c}M^c_{xy,x}=I_2^t\ddot{\theta}_y^t-\frac{h_t}{2h_c}I_2^c\ddot{\theta}_y^c\\&\delta w: \sum_i^{i=t,c,b}Q^i_{x,x}+Q^i_{y,y}+(N_{xm}+N_{xe}+N_{xa})w_{,xx}+(N_{ym}+N_{ye}+N_{ya})w_{,yy}=\sum_i^{i=t,c,b}I_0^i\ddot{w}\\&\frac{\partial D_z^{t,b}}{\partial z}=0\\&\frac{\partial B_z^{t,b}}{\partial z}=0\end{aligned}\tag{8}$$

In the above equations, forces and torques can be determined from:

$$\begin{Bmatrix}Q_x\\Q_y\end{Bmatrix}=k\int_{h/2}^{-h/2}\begin{Bmatrix}\tau_{xz}\\\tau_{yz}\end{Bmatrix}dz\qquad\begin{Bmatrix}I_0\\I_2\end{Bmatrix}=\int_{h/2}^{-h/2}\begin{Bmatrix}1\\z^2\end{Bmatrix}\rho(z)\,dz$$

$$\begin{Bmatrix}M_x\\M_y\\M_{xy}\end{Bmatrix}=\int_{h/2}^{-h/2}\begin{Bmatrix}\sigma_x\\\sigma_y\\\tau_{xy}\end{Bmatrix}z\,dz\qquad\begin{aligned}&N_{xm}=P\\&N_{ym}=\lambda P\\&N_{xe}=N_{ye}=E_{11}\varphi_0\\&N_{xa}=N_{ya}=F_{11}\psi_0\end{aligned}\tag{9}$$

where $N_{xm}, N_{xe}, N_{xa}, N_{ym}, N_{ye}$ and N_{ya} denote the mechanical, electrical and magnetic forces in the directions of *x* and *y*, respectively. By substituting the strain Eqs. (3) in the last two equations of Eq. (8) and solving the algebraic equations, Eq. (10) is obtained as:

© 2021 IAU, Arak Branch

$$E_{11}\Delta - E_{22}\frac{\partial^2\varphi}{\partial z^2} - E_{33}\frac{\partial^2\psi}{\partial z^2} = 0$$
$$F_{11}\Delta - E_{33}\frac{\partial^2\varphi}{\partial z^2} - F_{22}\frac{\partial^2\psi}{\partial z^2} = 0 \tag{10}$$

Now, using the Cramer's rule and integrating the Eq. (10), we have:

$$\frac{\partial\varphi}{\partial z} = \mathrm{H}_1 z\ \Delta + \frac{\varphi_0}{h}$$
$$\frac{\partial\psi}{\partial z} = \mathrm{H}_2 z\ \Delta + \frac{\psi_0}{h} \tag{11}$$
$$\Delta = \theta_{x,x} + \theta_{y,y}$$

By the substitution of Eqs. (3) and (11) in Eq. (9) and rewriting Eqs. (8), the equations of motion of the sandwich structure with the flexible core are extracted in the following form:

$$\left(\frac{KA^c_{55}h_b}{2h_c} - KA_{55}\right)w_{0,x} + \left(D_{11} + E_{12}\mathrm{H}_1 + F_{12}\mathrm{H}_2 + \frac{D^c_{11}h_b^2}{4h_c^2}\right)\theta^b_{x,xx}$$
$$+\left(D_{12} + D_{66} + E_{12}\mathrm{H}_1 + F_{12}\mathrm{H}_2 + \frac{D^c_{12}h_b^2}{4h_c^2} + \frac{D^c_{66}h_b^2}{4h_c^2}\right)\theta^b_{y,xy} - \frac{KA^c_{55}h_bh_t}{4h_c^2}\theta^t_x + \frac{D^c_{11}h_bh_t}{4h_c^2}\theta^t_{x,xx}$$
$$-\left(\frac{KA^c_{55}h_b^2}{4h_c^2} + KA_{55}\right)\theta^b_x + \left(\frac{D^c_{66}h_b^2}{4h_c^2} + D_{66}\right)\theta^b_{x,yy} + \frac{D^c_{66}h_bh_t}{4h_c^2}\theta^t_{x,yy} + \left(\frac{D^c_{66}h_bh_t}{4h_c^2} + \frac{D^c_{12}h_bh_t}{4h_c^2}\right)\theta^t_{y,xy} \tag{12a}$$
$$= I^b_2\ddot{\theta}^b_x + I^c_2\frac{h_b^2}{4h_c^2}\ddot{\theta}^b_x + I^c_2\frac{h_bh_t}{4h_c^2}\ddot{\theta}^t_x$$

$$\left(D_{12} + D_{66} + E_{12}\mathrm{H}_1 + F_{12}\mathrm{H}_2 + \frac{D^c_{12}h_b^2}{4h_c^2}\frac{D^c_{66}h_b^2}{4h_c^2}\right)\theta^b_{x,xy} - \left(KA_{44} + \frac{KA^c_{44}h_b}{2h_c}\right)w_{0,y}$$
$$+\left(D_{22} + E_{12}\mathrm{H}_1 + F_{12}\mathrm{H}_2 + \frac{D^c_{22}h_b^2}{4h_c^2}\right)\theta^b_{y,yy} + \frac{D^c_{22}h_bh_t}{4h_c^2}\theta^t_{y,yy} + \frac{D^c_{66}h_b^2}{4h_c^2}\theta^b_{y,xx} + \frac{D^c_{66}h_bh_t}{4h_c^2}\theta^t_{y,xx} + D_{66}\theta^b_{y,xx} \tag{12b}$$
$$-\left(KA_{44} + \frac{KA^c_{44}h_b^2}{4h_c^2}\right)\theta^b_y - \frac{KA^c_{44}h_bh_t}{4h_c^2}\theta^t_y + \left(\frac{D^c_{12}h_bh_t}{4h_c^2} + \frac{D^c_{66}h_bh_t}{4h_c^2}\right)\theta^t_{x,xy} = I^b_2\ddot{\theta}^b_y + I^c_2\frac{h_b^2}{4h_c^2}\ddot{\theta}^b_y + I^c_2\frac{h_bh_t}{4h_c^2}\ddot{\theta}^t_y$$

$$\left(D_{11} + E_{12}\mathrm{H}_1 + F_{12}\mathrm{H}_2 + \frac{D^c_{11}h_t^2}{4h_c^2}\right)\theta^t_{x,xx} + \left(\frac{D^c_{66}h_t^2}{4h_c^2} + D_{66}\right)\theta^t_{x,yy} + \frac{D^c_{11}h_bh_t}{4h_c^2}\theta^b_{x,xx}$$
$$+\left(D_{12} + D_{66} + E_{12}\mathrm{H}_1 + F_{12}\mathrm{H}_2 + \frac{D^c_{12}h_t^2}{4h_c^2} + \frac{D^c_{66}h_t^2}{4h_c^2}\right)\theta^t_{y,xy} + \frac{D^c_{12}h_bh_t}{4h_c^2}\theta^b_{y,xy} - \frac{KA^c_{55}h_bh_t}{4h_c^2}\theta^b_x$$
$$-\left(\frac{KA^c_{55}h_t^2}{4h_c^2} + KA_{55}\right)\theta^t_x + \left(\frac{KA^c_{55}h_t}{2h_c} - KA_{55}\right)w_{0,x} + \frac{D^c_{66}h_bh_t}{4h_c^2}\theta^b_{x,yy} + \frac{D^c_{66}h_bh_t}{4h_c^2}\theta^b_{y,xy} \tag{12c}$$
$$= I^t_2\ddot{\theta}^t_x + I^c_2\frac{h_bh_t}{4h_c^2}\ddot{\theta}^b_x + I^c_2\frac{h_t^2}{4h_c^2}\ddot{\theta}^t_x$$

© 2021 IAU, Arak Branch

$$\begin{aligned}
&\left(D_{12}+D_{66}+E_{12}\mathrm{H}_1+F_{12}\mathrm{H}_2+\frac{D_{12}^c h_t^2}{4h_c^2}+\frac{D_{66}^c h_t^2}{4h_c^2}\right)\theta_{x,xy}^t-\left(\frac{KA_{44}^c h_t^2}{4h_c^2}+KA_{44}\right)\theta_y^t\\
&+\left(D_{22}+E_{12}\mathrm{H}_1+F_{12}\mathrm{H}_2+\frac{D_{22}^c h_t^2}{4h_c^2}\right)\theta_{y,yy}^t+\left(\frac{KA_{44}^c h_t}{2h_c}-KA_{44}\right)w_{0,y}-\frac{KA_{44}^c h_b h_t}{4h_c^2}\theta_y^b\\
&D_{66}\theta_{y,xx}^t+\left(\frac{D_{12}^c h_b h_t}{4h_c^2}+\frac{D_{66}^c h_b h_t}{4h_c^2}\right)\theta_{x,xy}^b+\frac{D_{22}^c h_b h_t}{4h_c^2}\theta_{y,yy}^b+\frac{D_{66}^c h_b h_t}{4h_c^2}\theta_{y,xx}^b+\frac{D_{66}^c h_t^2}{4h_c^2}\theta_{y,xx}^t\\
&=I_2^t\ddot{\theta}_y^t+I_2^c\frac{h_b h_t}{4h_c^2}\ddot{\theta}_y^b+I_2^c\frac{h_t^2}{4h_c^2}\ddot{\theta}_y^t
\end{aligned}\tag{12d}$$

$$\begin{aligned}
&\left(KA_{44}-\frac{KA_{44}^c h_t}{2h_c}\right)\theta_{y,y}^t+\left(KA_{44}-\frac{KA_{44}^c h_b}{2h_c}\right)\theta_{y,y}^b+\left(KA_{55}-\frac{KA_{55}^c h_t}{2h_c}\right)\theta_{x,x}^t+\left(KA_{55}-\frac{KA_{55}^c h_b}{2h_c}\right)\theta_{x,x}^b\\
&+(2KA_{55}+KA_{55}^c+N_{xm}+N_{xe}+N_{xa})w_{0,xx}+(2KA_{44}+KA_{44}^c+N_{ym}+N_{ye}+N_{ya})w_{0,yy}=\left(I_0^t+I_0^c+I_0^b\right)\ddot{w}
\end{aligned}\tag{12e}$$

4 ANALYTIC SOLUTIONS FOR FREE VIBRATION RESPONSE AND BUCKLING OF THE SANDWICH STRUCTURE

The analytic solution of Eqs. (12) for the MEE sandwich panel under various boundary conditions will be constructed. The plate is assumed to have simply-supported (S), clamped (C) or free (F) edges or have combinations of them, they are given as[34, 35]:

Simply supported (s):

$$\begin{aligned}
&w_0=\theta_x=M_y=0 \quad at\ \ (y=0,b)\\
&w_0=\theta_y=M_x=0 \quad at\ \ (x=0,a)
\end{aligned}\tag{13}$$

Clamped (C):

$$w_0=\theta_x=\theta_y=0 \quad at\ \ (x=0,a)\ \&\ (y=0,b)\tag{14}$$

Free (F):

$$\begin{aligned}
&M_y=M_{xy}=Q_y=0 \quad at\ \ (y=0,b)\\
&M_x=M_{xy}=Q_x=0 \quad at\ \ (x=0,a)
\end{aligned}\tag{15}$$

To satisfy the above boundary conditions, following responses are being considered [34, 35]:

$$\begin{aligned}
&w_0(x,y,t)=W_{nm}X_n(x)Y_m(y)e^{i\omega t}\\
&\theta_x(x,y,t)=X_{nm}\frac{\partial X_n(x)}{\partial x}Y_m(y)e^{i\omega t}\\
&\theta_y(x,y,t)=Y_{nm}X_n(x)\frac{\partial Y_m(y)}{\partial y}e^{i\omega t}
\end{aligned}\tag{16}$$

where the functions $X_n(x)$ and $Y_m(y)$ are presented as bellow for considered boundary conditions:

© 2021 IAU, Arak Branch

$$\begin{aligned} &SS: \ X_n(x) = \mathrm{Sin}(\alpha x) \\ &CS: \ X_n(x) = \mathrm{Sin}(\alpha x)\left(\mathrm{Cos}(\alpha x) - 1\right) \\ &CC: \ X_n(x) = \mathrm{Sin}^2(\alpha x) \\ &FF: \ X_n(x) = \mathrm{Cos}^2(\alpha x)\left(\mathrm{Sin}^2(\alpha x) + 1\right) \end{aligned} \tag{17}$$

$$\begin{aligned} &SS: \ Y_m(y) = \mathrm{Sin}(\beta y) \\ &CS: \ Y_m(y) = \mathrm{Sin}(\beta y)\left(\mathrm{Cos}(\beta y) - 1\right) \\ &CC: \ Y_m(y) = \mathrm{Sin}^2(\beta y) \\ &FF: \ Y_m(y) = \mathrm{Cos}^2(\beta y)\left(\mathrm{Sin}^2(\beta y) + 1\right) \end{aligned} \tag{18}$$

where $\left(\alpha = \frac{n\pi}{a}\right)$ and $\left(\beta = \frac{m\pi}{b}\right)$. Moreover X_{nm},Y_{nm} and W_{nm} are arbitrary parameters and $\omega = \omega_{nm}$ denotes the Eigen frequency associated with (*nth, mth*) Eigen modes. The functions $X_n(x)$ and $Y_m(y)$ are suggested here to satisfy at least the geometric boundary conditions given in Eqs. (13)–(15), and represent approximate shapes of the deflected surface of the plate. Substituting expressions (16) into the governing Eqs. (12) and multiplying each equation by the corresponding Eigen function then integrating over the domain of solution, we can obtain, after some mathematical manipulations, the following equations:

$$\left\{[M]\omega^2 - [K]\right\}[q] = 0 \tag{19}$$

where, *M* is the mass matrix and *K* is the stiffness matrix. In order to analyze the buckling of the structure, the kinetic energy relations are eliminated and Eq. (16) is substituted in the PDE of Eq. (12); hence the algebraic equations would be obtained in the form of Eq. (20):

$$\{[K]\}[q] = 0 \tag{20}$$

In the above relation, *K* is a 5×5 square matrix in terms of the unknown *p*, by solving which the amount of buckling load can be calculated.

5 VALIDATION

Since the buckling and vibrations of the MEE sandwich structure with a flexible core has not been studied yet, for the sake of validation, the results of buckling and vibration of the single-layer MEE plate was compared with the results provided by Lee and Zhang [29, 30]. Finally, the vibrations of the sandwich structure was compared with the work of Yang et al. [36]. The values of dimensionless natural frequency of the single-layer MEE plate is provided in Table 1. The thickness-to-length ratio of the plate was assumed as 0.01 and the elastic substrate and magnetic potential terms were considered to be zero. In addition, the dimensionless relation of frequency was defined as $\chi = \frac{\omega a^2}{h}\sqrt{\frac{\rho}{c_{11}}}$. As can be seen, there is a good match between the results.

Table 1
Comparison of the natural frequencies of the MEE plate.

	a/b	$\varphi_0 = -10^5(v)$	$\varphi_0 = 0$	$\varphi_0 = 10^5(v)$
Present	1	7.15	5.66	3.58
Li & Zhang[20]		7.16	5.66	3.58
Present	2	15.63	14.01	12.18
Li & Zhang[20]		15.64	14.02	12.19

© 2021 IAU, Arak Branch

The dimensionless critical load values of the single-layer MEE plate for different ratio of thickness to length are listed in Table 2. The elastic substrate and electrical and magnetic potentials were considered to be zero. The dimensionless relationship of critical load was also defined as $P_{cr} = \frac{p\,a^2}{h^3 c_{11}}$. As can be seen, there is a good match between the results.

Table 2
Comparison of the buckling load of the MEE plate.

	λ	$h/a = 0.1$	$h/a = 0.15$	$h/a = 0.2$
Present	0	2.94	2.63	2.32
Li [22]		2.97	2.67	2.33
Present	0.5	1.98	1.78	1.54
Li [22]		1.99	1.79	1.55

The vibrations of the sandwich structure provided in Table 3 are compared with the work of Yang et al. [36] for the first four frequencies. The upper and lower plates were made of aluminum and the core was made of viscoelastic with a complex Young's modulus. The core thickness was 2 times of the thickness of lower and upper layers and the ratio of length to thickness was assumed to be 100. Additionally, square plate with a length and width of 1 meter was considered. Moreover, the dimensionless relationship of the plate was defined as $\chi = \frac{\omega a^2}{h}\sqrt{\frac{\rho_0}{E_0}}$. The closeness of the results confirms the accuracy of the present method.

Table 3
Comparison of the dimensionless natural frequency of the isotropic sandwich panel with flexible core.

$a/h = 100 \quad a = b$	ω_{22}	ω_{21}	ω_{12}	ω_{11}
Yang et al.[36]	6.440	4.434	4.434	2.350
Present work	6.386	4.362	4.362	2.297

6 RESULTS AND DISCUSSIONS

In this section, the obtained results of vibration and buckling of MEE sandwich plates with flexible cores are discussed. The top and bottom layers were made of MEE and the core was made of flexible foam. The properties of MEE material and core materials are given in Table 4. The effect of electric potential on the natural frequency for different ratios of width to different lengths is represented in Fig. 2.

Table 4
The properties of different materials.

MEE material properties [28]			
$C_{11}\,(Gpa)$	226	$C_{22}\,(Gpa)$	216
C_{12}	125	$C_{44} = C_{55}$	44.2
C_{66}	50.5	$e_{31}\ \ (C/m^2)$	-2.2
$q_{31}(N/MA)$	290.1	η_{33}	-297
μ_{33}	275	d_{33}	2737.5
$\rho(kg/m^3)$	5550		
Core material properties [36]			
$E_{11} = E_{22}\ \ (Gpa)$	0.5776	$G_{12}\,(Gpa)$	0.1079
ν_{12}	0.0025	$\rho(kg/m^3)$	1000

© 2021 IAU, Arak Branch

As can be seen in this figure, the total thickness of the structure and the thickness to the length ratio of the plate is 0.2 and the thickness of the upper and lower layers is 2 times of the thickness of core. According to this figure, the natural frequency of the plate decreases with increasing the electric potential and the ratio of width to length of the plate. Due to the negative values of electrical coefficients of MEE plates, the values of stiffness matrix increased by applying negative potential to the system, which was followed by an increase in the natural frequency. In contrast, if the positive electric potential was applied to the plate, the stiffness matrix would be decreased with the subsequent decrease in the natural frequency of the structure. In addition, by increasing the width-to-length ratio of the plate, reduced stiffness and the consequent decreased natural frequency would be achieved.

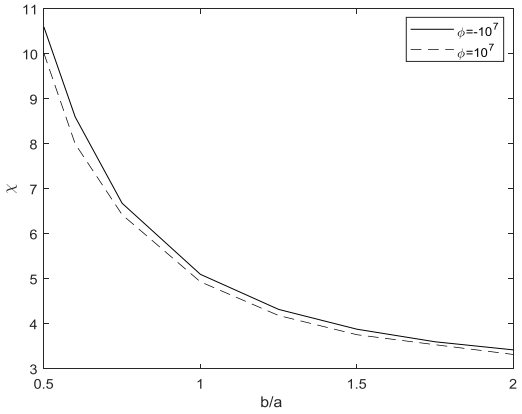

Fig.2
The effect of electric potential of the sandwich panel on the natural frequency of the system.

In Tables 5, the dimensionless frequency of MEE sandwich panels are presented, respectively, accounting for different kinds of boundary conditions (SSSS, CSSS, CSCS,CCCC, and FFCC) for various electric voltages at *a/h* = 100, *a/h* = 20, and *a/h* = 10. According to these tables as the thickness rises, the dimensionless frequency rises. Also, it is concluded that by increasing the thickness of the sandwich panel, the effect of electrical potential decreases on the dimensionless frequency. Moreover, it is found that for all kinds of boundary conditions, negative values of electric voltage provide higher frequencies than positive values. This is due to the axial compressive and tensile forces produced in the MEE sandwich plate by the applied positive and negative voltages, respectively. Therefore, the sign of applied voltage shows a prominent impact on the vibrational responses of MEE sandwich plates.

Table 5
Variation of dimensionless frequency of MEE sandwich plate for various boundary conditions and electric voltages.

B.C	φ	$a=b=100h \quad h=2h_c$	$a=b=20h \quad h=2h_c$	$a=b=10h \quad h=2h_c$
SSSS	-10^6	38.7175	7.836	6.5064
	0	14.03	7.145	6.4073
	10^6	8.1621	6.378	6.3066
CSSS	-10^6	43.548	10.570	8.842
	0	17.082	9.913	8.74
	10^6	10.457	9.346	8.587
CSCS	-10^6	49.768	12.926	10.88
	0	19.841	12.270	10.679
	10^6	14.241	11.984	10.432
CCCC	-10^6	45.8509	13.071	10.786
	0	19.1356	12.5326	10.707
	10^6	13.8765	12.470	10.69
CCFF	-10^6	46.977	13.620	11.08
	0	19.428	13.131	11.01
	10^6	14.017	12.569	10.83

The effect of magnetic potential on the natural frequency for different ratios of width to lengths is plotted in Fig. 3. In the desired configuration, the total thickness of the structure and the thickness to the length ratio is 0.2 and the thickness of the core is 2 times of the thickness of the upper and lower layers. As can be seen, by reducing the magnetic potential and increasing the ratio of width to length, a reducing trend can be seen in the natural frequency of the plate. Regarding the positive values of magnetic coefficients of MEE plates, application of negative potential to the system

© 2021 IAU, Arak Branch

would resulted in a reduction in the values of stiffness matrix and the consequent decrease in the natural frequency. Moreover, by the application of a positive magnetic potential to the plate, the stiffness matrix was increased, which was followed by an increase in the natural frequency of the structure. The common feature that can be deduced by the comparison of Fig. 2 and 3, is the insignificant effect of electric and magnetic potentials on the natural frequency. However, these effects should be considered in the investigations.

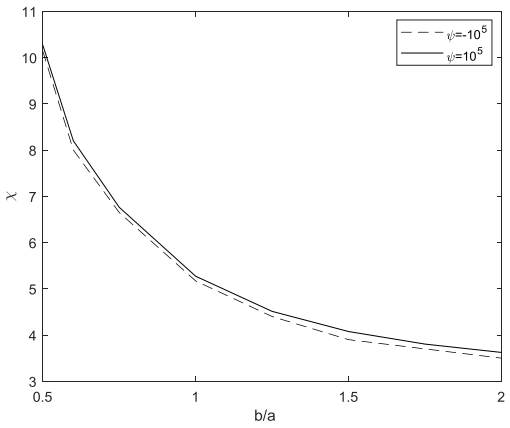

Fig.3
The effect of magnetic potential of the sandwich panel on the natural frequency of the system.

The variation of natural frequency of the system with the thickness of the sandwich plate core is represented in Fig. 4. The considered configuration in this figure was a 1×1 square plate with the total thickness of 0.2. As can be seen in the figure, with the increase of core thickness, first an increasing trend can be seen for the natural frequency, which was followed by the decreasing one. The reason for the initial increase in natural frequency is attributed to the decrease in the amount of mass matrix. Considering the constant total thickness for the sandwich structure, by increasing the core thickness, the thickness of the upper and lower MEE layers would be decreased, which leads to lightening of the structure and reduction of the mass matrix. By further increasing the ratio of core thickness to total thickness after 0.5, the effect of mass matrix is dominated by the increase of structure stiffness, and as a consequence, the natural frequency of the system decreases.

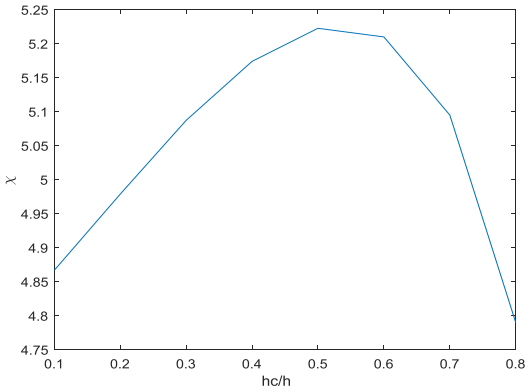

Fig.4
The effect of flexible core thickness of the sandwich panel on the natural; frequency of the system.

The buckling behavior of the sandwich plate is plotted for different length-to-width ratios in Fig. 5. The thickness of all three layers was considered to be the same value of 0.1. The buckling load is drawn for two modes, in which, the parameter λ is associated with the applied load. As can be seen, as the length-to-width ratio increases, the critical load is increased. It should be noted that this increase would be much greater if the load is applied only along the length compared to the case that the half of the load is applied along the width of the plate. The variation of buckling behavior with electric and magnetic potentials is displayed in Figs. 6 and 7. According to Fig. 6, the reducing trend of critical load by increasing the electrical potential is evident.

© 2021 IAU, Arak Branch

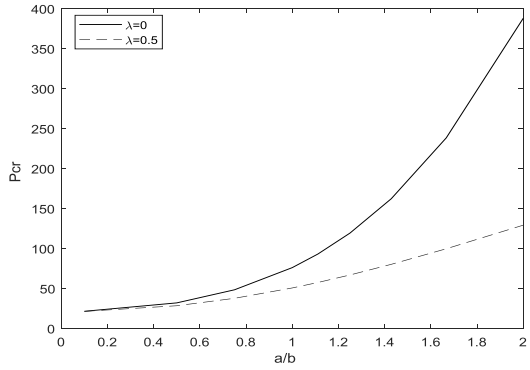

Fig.5
The effect of length-to width ratio of the sandwich panel on the critical load.

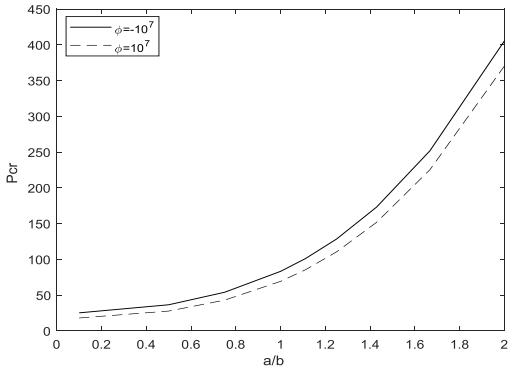

Fig.6
The effect of electric potential of the sandwich panel on the critical load.

As shown in Fig. 7, the critical load of the structure increases with increasing magnetic potential. The effect of increasing the core thickness on the critical load for the values of λ equal to zero and 0.5 is illustrated in Fig. 8. Regarding this figure, an increasing behavior of the critical load can be observed by increasing the core thickness.

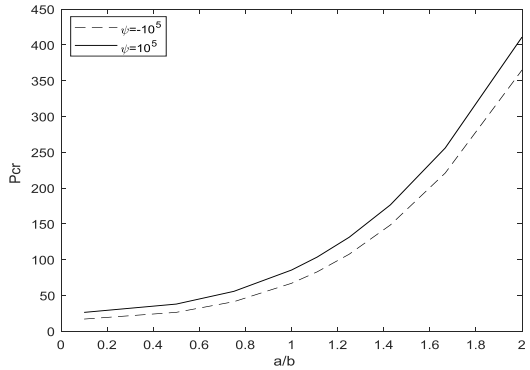

Fig.7
The effect of magnetic potential of the sandwich panel on the critical load.

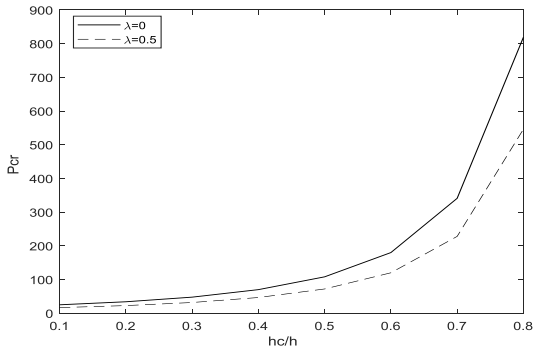

Fig.8
The effect of core thickness of the sandwich panel on the critical load.

© 2021 IAU, Arak Branch

7 CONCLUSION

In this paper, the buckling and free vibrations of a MEE sandwich panel with a flexible core were investigated. The governing equations of motion for the desired panel were derived based on the first-order shear deformation theory using the Hamilton's principle, and the obtained PDEs were solved for all kind of boundary condition. The considered assumptions of this study were the neglection of the in-plane electric and magnetic potentials, as well as displacement of the mid-plates. According to the obtained results, in MEE sandwich panel, the electric potential was inversely related to the natural frequency and buckling load, so that with increasing the electric potential, the natural frequency and critical load of the structure were also increased. Moreover, the magnetic potential was directly related to the natural frequency and buckling load of the system, and increasing trends of natural frequency and critical load were observed by increasing the magnetic potential. It should be noted that the effect of electric and magnetic potentials on plate buckling was much greater than their effect on the natural frequency of the structure. It is observed from table 5 that at a defined voltage, the FFCC MEE sandwich panel has the highest natural frequency then followed by CSCS, CCCC, CSSS and SSSS, respectively. Thus, for more accurate design of smart MEE sandwich panels, it is essential to consider various boundary conditions. Additionally, it was found that further increase in the core thickness greater than the λ ratio of 0.5 was resulted in a decrease in the natural frequency of the system. Moreover, the buckling load was decreased with increasing transverse load in the structure, which was much more pronounced for the length-to-width ratio higher than one. On the other hand, by increasing the thickness of the flexible core relative to the total thickness, the effect of transverse buckling load on the structure was increased. For further study, nonlinear analysis with viscoelastic core will be considered.

APPENDIX

$$D_{11}=\int_{-h/2}^{h/2}C_{11}z^{2}dz \qquad D_{12}=\int_{-h/2}^{h/2}C_{12}z^{2}dz \qquad D_{22}=\int_{-h/2}^{h/2}C_{22}z^{2}dz \qquad D_{66}=\int_{-h/2}^{h/2}C_{66}z^{2}dz$$

$$A_{44}=\int_{-h/2}^{h/2}C_{44}dz \qquad A_{55}=\int_{-h/2}^{h/2}C_{55}dz$$

$$E_{11},E_{12}=\int_{-h/2}^{h/2}e_{31}\,(1,z^{2})\,dz \qquad E_{22}=\int_{-h/2}^{h/2}\eta_{33}\,dz \qquad E_{33}=\int_{-h/2}^{h/2}d_{33}\,dz$$

$$F_{11},F_{12}=\int_{-h/2}^{h/2}q_{31}\,(1,z^{2})\,dz \qquad F_{22}=\int_{-h/2}^{h/2}\mu_{33}\,dz$$

$$\mathrm{H}_1=\frac{E_{11}F_{22}-E_{33}F_{11}}{E_{22}F_{22}-E_{33}^{2}} \qquad \mathrm{H}_2=\frac{E_{11}E_{33}-E_{22}F_{11}}{E_{22}F_{22}-E_{33}^{2}}$$

REFERENCES

[1] Plantema F., 1966, *Sandwich Construction*, New York, John Wiley and Sons.

[2] Allen H.G., 2013, *Analysis and Design of Structural Sandwich Panels: The Commonwealth and International Library: Structures and Solid Body Mechanics Division*, Elsevier.

[3] Rais-Rohani M., Marcellier P.,1999, Buckling and vibration analysis of composite sandwich plates with elastic rotational edge restraints,*AIAA Journal* **37**(5): 579-587.

[4] Frostig Y., Thomsen O.T., 2004, High-order free vibration of sandwich panels with a flexible core, *International Journal of Solids and Structures* **41**(5-6): 1697-1724.

[5] Frostig Y., 1998, Buckling of sandwich panels with a flexible core—high-order theory, *International Journal of Solids and Structures* **35**(3-4): 183-204.

[6] Schwarts-Givli H., Rabinovitch O., Frostig Y., 2007, Free vibrations of delaminated unidirectional sandwich panels with a transversely flexible core—a modified Galerkin approach, *Journal of Sound and Vibration* **301**(1-2): 253-277.

[7] Schwarts-Givli H., Rabinovitch O., Frostig Y., 2008, Free vibration of delaminated unidirectional sandwich panels with a transversely flexible core and general boundary conditions—A high-order approach, *Journal of Sandwich Structures & Materials* **10**(2): 99-131.

[8] Frostig Y., Thomsen O.T., 2009, On the free vibration of sandwich panels with a transversely flexible and temperature-dependent core material–Part I: Mathematical formulation,*Composites Science and Technology* **69**(6): 856-862.

[9] Frostig Y., Thomsen O.T., 2009, On the free vibration of sandwich panels with a transversely flexible and temperature dependent core material–part II: numerical study,*Composites Science and Technology* **69**(6): 863-869.

© 2021 IAU, Arak Branch

[10] Araújo A.L., Carvalho V.S., Mota Soares C.M., Belinha J., Ferreira A.J.M., 2016, Vibration analysis of laminated soft core sandwich plates with piezoelectric sensors and actuators,*Composite Structures* **151**: 91-98.

[11] Malekzadeh Fard K., Payganeh G., Kardan M., 2013, Dynamic response of sandwich panels with flexible cores and elastic foundation subjected to low-velocity impact ,*Amirkabir Journal of Science & Research (Mechanical Engineering)* **45**(2): 27-42.

[12] Malekzadeh Fard K., Malek M.H., 2017, Free vibration and buckling analysis of sandwich panels with flexible cores using an improved higher order theory, *Journal of Solid Mechanics* **9**(1): 39-53.

[13] Daikh A.A., Drai A., Bensaid I., Houari M.S.A., Tounsi A., 2020, On vibration of functionally graded sandwich nanoplates in the thermal environment, *Journal of Sandwich Structures & Materials* doi.org/10.1177/1099636220909790**.**

[14] Jam J., Eftari B., Taghavian S., 2010, A new improved high-order theory for analysis of free vibration of sandwich panels, *Polymer Composites* **31**(12): 2042-2048.

[15] Mohammadimehr M., Mostafavifar M., 2016, Free vibration analysis of sandwich plate with a transversely flexible core and FG-CNTs reinforced nanocomposite face sheets subjected to magnetic field and temperature-dependent material properties using SGT,*Composites Part B: Engineering* **94**: 253-270.

[16] Kumar P., Srinivasa C., 2018, On buckling and free vibration studies of sandwich plates and cylindrical shells: a review, *Journal of Thermoplastic Composite Materials* **33**: 673-724.

[17] Pan E., Heyliger P.R., 2002, Free vibrations of simply supported and multilayered magneto-electro-elastic plates, *Journal of Sound and Vibration* **252**(3): 429-442.

[18] Buchanan G.R., 2004, Layered versus multiphase magneto-electro-elastic composites, *Composites Part B: Engineering* **35**(5): 413-420.

[19] Chen W.Q., Lee K.Y., Ding H.J., 2005, On free vibration of non-homogeneous transversely isotropic magneto-electro-elastic plates, *Journal of Sound and Vibration* **279**: 237-251.

[20] Ramirez F., Heyliger P.R., Pan E., 2006, Free vibration response of two-dimensional magneto-electro-elastic laminated plates, *Journal of Sound and Vibration* **292**(3-5): 626-644.

[21] Liu M.-F., Chang T.-P., 2010, Closed form expression for the vibration problem of a transversely isotropic magneto-electro-elastic plate ,*Journal of Applied Mechanics* **77**(2): 024502.

[22] Davì G., Milazzo A., 2011, A regular variational boundary model for free vibrations of magneto-electro-elastic structures, *Engineering Analysis with Boundary Elements* **35**(3): 303-312.

[23] Milazzo A., Orlando C., 2012, An equivalent single-layer approach for free vibration analysis of smart laminated thick composite plates,*Smart Materials and Structures* **21**(7): 075031.

[24] Chang T.P., 2013, On the natural frequency of transversely isotropic magneto-electro-elastic plates in contact with fluid, *Applied Mathematical Modelling* **37**(4): 2503-2515.

[25] Chang T.P., 2013, Deterministic and random vibration analysis of fluid-contacting transversely isotropic magneto-electro-elastic plates,*Computers & Fluids* **84**: 247-254.

[26] Chen J.Y., Heyliger P.R., Pan E., 2014, Free vibration of three-dimensional multilayered magneto-electro-elastic plates under combined clamped/free boundary conditions, *Journal of Sound and Vibration* **333**(17): 4017-4029.

[27] Kattimani S.C., Ray M.C., 2014, Smart damping of geometrically nonlinear vibrations of magneto-electro-elastic plates,*Composite Structures* **114**: 51-63.

[28] Ke L.-L., Wang Y.-S., Yang J., Kitipornchai S., 2014, Free vibration of size-dependent magneto-electro-elastic nanoplates based on the nonlocal theory,*Acta Mechanica Sinica* **30**(4): 516-525.

[29] Li Y., Zhang J., 2014, Free vibration analysis of magnetoelectroelastic plate resting on a Pasternak foundation,*Smart Materials and Structures* **23**(2): 025002.

[30] Li Y.S., 2014, Buckling analysis of magnetoelectroelastic plate resting on Pasternak elastic foundation, *Mechanics Research Communications* **56**: 104-114.

[31] Karimi M., Farajpour M.R., Rafieian S., Milani A.S., Khayyam H., 2020, Surface energy layers investigation of intelligent magnetoelectrothermoelastic nanoplates through a vibration analysis, *The European Physical Journal Plus* **135**(6): 488.

[32] Karimi M., Shahidi A.R., 2019, A general comparison the surface layer degree on the out-of-phase and in-phase vibration behavior of a skew double-layer magneto–electro–thermo-elastic nanoplate, *Applied Physics A* **125**(2): 106.

[33] Karimi M., Shahidi A.R., 2019, Comparing magnitudes of surface energy stress in synchronous and asynchronous bending/buckling analysis of slanting double-layer METE nanoplates, *Applied Physics A* **125**(2): 154.

[34] Barati M.R., Shahverdi H., Zenkour A.M., 2017, Electro-mechanical vibration of smart piezoelectric FG plates with porosities according to a refined four-variable theory, *Mechanics of Advanced Materials and Structures* **24**(12): 987-998.

[35] Thai H.-T., Choi D.-H., 2012, A refined shear deformation theory for free vibration of functionally graded plates on elastic foundation,*Composites Part B: Engineering* **43**(5): 2335-2347.

[36] Yang C., Jin G., Ye X., Liu Z., 2016, A modified Fourier–Ritz solution for vibration and damping analysis of sandwich plates with viscoelastic and functionally graded materials, *International Journal of Mechanical Sciences* **106**: 1-18.

© 2021 IAU, Arak Branch